Structure, luminescence and scintillation properties of the $MgWO_4$–$MgMoO_4$ system

2008 J. Phys.: Condens. Matter 20 365219

(http://iopscience.iop.org/0953-8984/20/36/365219)

J. Phys.: Condens. Matter **20** (2008) 365219 (8pp) doi:10.1088/0953-8984/20/36/365219

Structure, luminescence and scintillation properties of the $MgWO_4$–$MgMoO_4$ system

V B Mikhailik[1,5], H Kraus[1], V Kapustyanyk[2], M Panasyuk[2], Yu Prots[3], V Tsybulskyi[2] and L Vasylechko[4]

[1] Department of Physics, University of Oxford, Oxford OX1 3RH, UK
[2] Scientific-Technical and Educational Centre of Low Temperature Studies, I Franko National University of Lviv, 50 Dragomanova Street, 79005, Lviv, Ukraine
[3] Max-Planck-Institut für Chemische Physik fester Stoffe, Nöthnitzer Street 40, 01187 Dresden, Germany
[4] Semiconductor Electronics Department, Lviv Polytechnic National University, 12 Bandera Street, 79013, Lviv, Ukraine

E-mail: vmikhai@hotmail.com

Received 1 June 2008
Published 19 August 2008
Online at stacks.iop.org/JPhysCM/20/365219

Abstract

The importance of luminescent tungstates and molybdates in several technological applications motivated the study of the structural, luminescence and scintillation properties of the $MgWO_4$–$MgMoO_4$ system. X-ray diffraction studies allowed the identification of three main types of structures in the pseudo-binary $MgWO_4$–$MgMoO_4$ system (sanmartinite β-$MgMoO_4$, cuprosheelite α-$MgMoO_4$, and wolframite $MgWO_4$) and the refinement of the parameters of the crystal lattice. It is found that the single-phase solid solution $MgMo_{1-x}W_xO_4$ with a β-$MgMoO_4$ structure is created only at $x < 0.10$, while for a higher tungsten content a mixture of different phases is formed. The x-ray luminescence spectra of a series of samples of the $MgWO_4$–$MgMoO_4$ system are measured at $T = 8$ K. The principal emission bands are assigned to the main structural phases as follows: β-$MgMoO_4$, 520 nm; α-$MgMoO_4$, 590 nm; $MgWO_4$ (wolframite), 480 nm. The phase composition of the sample determines the actual shape of the observed spectra. Possible relations between the crystal structure and luminescence properties of different phases are discussed in terms of a configuration coordinate model. Of all the compounds under test, $MgWO_4$ is found to have the best scintillation response for particle excitation (0.90 ± 0.15 that of $ZnWO_4$ at $T = 295$ K). Further, the light yield also remains high with decreasing temperature, which makes this material potentially useful for cryogenic applications.

1. Introduction

Metal tungstates and molybdates of the general formula ABO_4 (A = Mg, Ca, Sr, Cd, Zn, Pb; B = Mo, W) have been studied extensively for decades, owing to their technological importance in a variety of applications such as phosphors [1], detectors of ionizing radiation [2, 3] or optoelectronic devices [4]. The optical and luminescence properties of materials are of particular significance in such applications, resulting in a significant amount of relevant information gathered by generations of scientists [5–12]. Research on these compounds intensified recently due to newly emerging applications. For example, the development of lead tungstate scintillation detectors for the Large Hadron Collider [13] motivated some of the research activities over the last decade. Extensive experimental and theoretical studies led to a better understanding of the nature and the major physical properties of the compounds that eventually furthered the optimization of lead tungstate scintillators [14].

The study of materials belonging to the tungstate and molybdate families received new impetus recently due to the

[5] Author to whom any correspondence should be addressed.

need to provide different scintillation targets for cryogenic particle physics experiments searching for rare events, such as interaction with dark matter particles [15, 16], neutrinoless double-beta decay [17] or radioactive decay of very long-lived nuclei [18, 19]. A major benefit arising from the use of scintillating crystals in such experiments is the possibility of identifying the type of particle interaction and to reject with high efficiency spurious events caused by the radioactive background. This is achieved through the simultaneous detection of the phonon and scintillation response produced in the target material by impinging particles or high-energy quanta [20, 21]. Thus, the identification, characterization and optimization of potentially useful scintillation materials for cryogenic applications is an important task, driven by the requirements of experiments searching for rare events.

Tungstates and molybdates can offer a detector target composition that is needed to address different experimental objectives. They are cryogenically compatible and can offer the variety of potential target materials needed to achieve the scientific goals of some experiments. A necessary requirement for a target material is that its phonon, scintillation and mechanical properties are suitable. Therefore an investigation of the low-temperature scintillation properties of these materials has recently attracted attention (see, e.g., review paper [22] and references therein).

Within this family of materials, magnesium tungstate and molybdate are of particular interest in the search for rare events. The presence of the light magnesium cation inhibits the tendency of the crystalline matrix to incorporate heavy radioactive nuclei and thereby reduces the inherent intrinsic radioactivity of the compound, compared with other representatives of the same family. Furthermore, $MgWO_4$ is known to be an efficient phosphor exhibiting intrinsic emission, which increases with decreasing temperature [8, 23]. Therefore it can be a very attractive complementary target to other tungstate scintillators in cryogenic searches for dark matter.

Equally, scintillators containing molybdenum are of significant interest for the detection of the neutrinoless double-beta decay of ^{100}Mo. $MgMoO_4$, exhibiting a luminescence intensity that is ∼30% that of $CaWO_4$ at $T = 8$ K [24] under photoexcitation, could have been the material of choice, but unfortunately no scintillation was detected from particle excitation [25]. It is known that in materials with intrinsic emission, the structure of the emission centre is a dominant factor, determining the luminescence efficiency [9, 23]. Given the excellent luminescence characteristics of $MgWO_4$ and the poor scintillator performance of $MgMoO_4$ it is worthwhile investigating the change of the physical properties with concentration in a system containing both W and Mo cations, and to find the correlation between structure and luminescence in the $MgMoO_4$–$MgWO_4$ system. This might eventually provide very instructive information for tailoring desirable material properties. Another motivation of this study is the characterization of suitable Mg-based compounds for application as cryogenic scintillators.

2. Experiment

A series of powder samples in a $(1 - x)MgMoO_4$–$xMgWO_4$ pseudo-binary system with x = 0, 0.01, 0.05, 0.1, 0.3, 0.5, 0.7, 0.9 and 1 were synthesized by a solid state reaction technique at 900 °C for 24 h, starting from mixtures of MgO, MoO_3 and WO_3 (not less than 4N purity) oxides. For phase analysis and crystallographic characterization a Huber image plate Guinier camera G670 with monochromatic Cu Kα1 radiation ($\lambda = 1.540\,56$ Å) was used. Silicon ($a = 5.431\,02$ Å) powder was applied as the internal standard for the precise refinement of the lattice parameters. Refinement of the lattice parameters and full-profile structure refinement were performed using the Windows version of the crystal structure determination program package WinCSD [26].

The experimental samples for scintillation studies were prepared in the following way. A small quantity of powder was placed on a 5 × 5 mm^2 glass substrate and mixed with a drop of acetone to produce a paste. After the acetone evaporated a smooth non-transparent powder film was formed on the substrate. The sample was placed into a He-flow optical cryostat and exposed to alpha particle excitation from a ^{241}Am source. The scintillation signal was detected using a green-sensitive photomultiplier (Electron Tubes model 9124) attached to the cryostat window. Measurements of variation of the scintillation response and decay time, with temperature, were carried out using the multiphoton counting (MPC) technique. A detailed description of the original experimental setup and the procedure of data analysis can be found in [27] and subsequent papers [28, 29], which describe the progressive improvements of this technique.

Measurements of x-ray luminescence were carried out in a helium cryostat designed for these studies. The cryostat contains quartz windows for light detection and a beryllium window for x-ray excitation of the samples. An x-ray tube with a Mo-anticathode operating at 55 kV and 10 mA was used as an excitation source. The contribution of the low-energy continuum was reduced by means of a 0.5 mm thick aluminium filter. The luminescence spectra were recorded through an MDR-12 monochromator with a band pass of 18 nm. A green-sensitive photomultiplier FEU-79 operating in the single-photon counting regime was used as a photodetector. The data presented here are not corrected for the spectral response of the detection system. Fortunately the influence of the spectral response of the setup on the measured luminescence characteristics is small and featureless in our region of interest (see section 4) and it is not an issue for comparative studies of the materials under investigation.

3. Characterization of the crystal structure

X-ray diffraction (XRD) examination of $MgMoO_4$ and Mo-rich $MgMo_{1-x}W_xO_4$ samples with $x = 0.01$, 0.05 and 0.1 revealed a monoclinic sanmartinite-type of structure, identical to β-$MgMoO_4$ given in the PDF-2 database (PDF cards 21-961 and 72-2153). There was no indication of peaks of a foreign phase. Full-profile Rietveld refinement of the lattice parameters, and the position and displacement of atoms

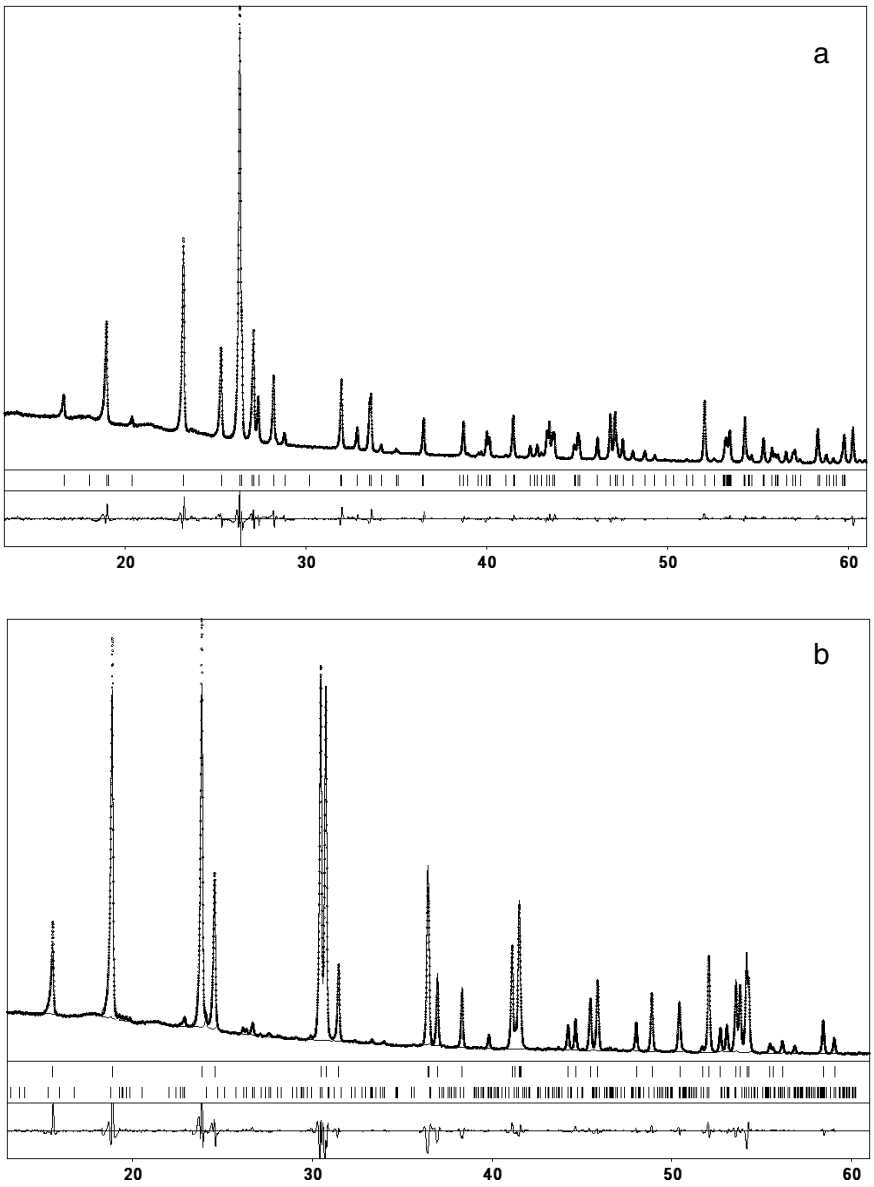

Figure 1. Graphical results of Rietveld refinement of $MgMo_{0.9}W_{0.1}O_4$ (top) and $MgMo_{0.1}W_{0.9}O_4$ (bottom) at room temperature (Cu Kα_1 radiation, $\lambda = 1.540\,56$ Å). Experimental (dots), calculated and difference curves as well as the positions of reflections are given. The $MgMo_{0.1}W_{0.9}O_4$ structure was refined in the two-phase mode.

performed in the space group $C2/m$ confirm the structure of $MgMo_{1-x}W_xO_4$ specimens with $x = 0$–0.1. The refinement of site occupancies shows a uniform distribution of Mo and W atoms over both the 4*h* and 4*i* tetrahedral sites in $MgMo_{1-x}W_xO_4$ structures. Final results of the Rietveld refinement of the $MgMo_{0.9}W_{0.1}O_4$ structure are presented in table 1 and figure 1 (top).

The tungsten-rich specimens $MgWO_4$ and $MgMo_{0.1}W_{0.9}O_4$ exhibit a wolframite-type structure, and only traces of the impurity phase were observed in the last sample. These extra peaks were assigned to the high-temperature (HT) α-phase of $MgMoO_4$ with triclinic structure (PDF card 31-796). Simultaneous two-phase Rietveld refinement of the pattern of the $MgMo_{0.1}W_{0.9}O_4$ specimen confirms wolframite- and α-$MgMoO_4$ cuproscheelite-type structures for the major and minor phases, respectively (figure 1, bottom). As the starting models for the refinement the atomic positions in $MgWO_4$ [30] and α-$ZnMoO_4$ [31] structures were taken. Final values for the structural parameters of the wolframite-type phase of $MgMo_{0.1}W_{0.9}O_4$ are presented in table 1. For the minor α-$MgMoO_4$ cuproscheelite-type phase only the lattice parameters were refined (see table 2).

Complex multi-phase compositions were found in the $MgMo_{1-x}W_xO_4$ samples with an intermediate Mo/W ratio ($x = 0.3$–0.7). Two major phases with cuprosheelite α-$MgMoO_4$ and wolframite β-$MgWO_4$ types of structures are found in $MgMo_{0.5}W_{0.5}O_4$ and $MgMo_{0.3}W_{0.7}O_4$ specimens in tentative proportions 7:2 and 2:7, respectively. In addition, a small amount of a third unidentified phase (less than 10 at.%) has been detected in both samples. In the sample with nominal composition $MgMo_{0.7}W_{0.3}O_4$ we identified two major phases, i.e. α- and β-modifications of $MgMoO_4$. In addition, a number

Table 1. Refined structural parameters of $MgMo_{0.9}W_{0.1}O_4$ and $MgMo_{0.1}W_{0.9}O_4$ structures at room temperature.

Atom	Site	x/a	y/b	z/c	B_{iso}	Occupations
$MgMo_{0.9}W_{0.1}O_4$, space group $C2/m$; $R_I = 0.0564$, $R_P = 0.1047$						
Mg1	4g	1/2	0.180 1(3)	0	1.01(6)	
Mg2	4i	0.800 4(3)	1/2	0.6410(4)	0.62(6)	
Mo1	4h	1/2	0.250 83(8)	1/2	0.52(1)	0.891(5)Mo + 0.109(5)W
Mo2	4i	0.729 36(8)	1/2	0.0961(1)	0.64(2)	0.892(5)Mo + 0.108(5)W
O1	8j	0.539 8(3)	0.150 0(4)	0.3081(5)	0.76(8)	
O2	8j	0.362 4(4)	0.351 9(4)	0.3869(5)	1.45(8)	
O3	4i	0.853 5(5)	1/2	−0.0427(7)	1.90(13)	
O4	8j	0.635 1(4)	0.351 1(4)	0.0344(5)	1.70(9)	
O5	4i	0.292 9(5)	0	0.3496(8)	1.77(13)	
$MgMo_{0.1}W_{0.9}O_4$, space group $P2/c$; $R_I = 0.0386$, $R_P = 0.0829$						
Mg	2f	1/2	0.670 7(4)	1/4	1.35(4)	
W	2*e*	0	0.181 69(6)	1/4	0.497(8)	0.9 + 0.1Mo
O1	4g	0.208 5(5)	0.107 6(5)	0.9426(6)	0.72(7)	
O2	4g	0.252 8(5)	0.366 3(5)	0.3996(6)	1.53(7)	

Table 2. Lattice parameters and cell volumes of different modifications of 'pure' and mixed magnesium molybdates and tungstates existing in the $MgMoO_4$–$MgWO_4$ pseudo-binary system.

Nominal composition	Str. type	a (Å)	b (Å)	c (Å)	α (deg)	β (deg)	γ (deg)	V (Å^3)	References
$MgMoO_4$	Sanmartinite	10.278 17(4)	9.292 13(6)	7.028 23(3)	90	106.889(1)	90	642.29(1)	This work
$MgMo_{0.99}W_{0.01}O_4$	Sanmartinite	10.280 18(7)	9.292 77(8)	7.029 83(4)	90	106.915(1)	90	642.52(2)	This work
$MgMo_{0.95}W_{0.05}O_4$	Sanmartinite	10.278 77(5)	9.292 43(7)	7.029 52(3)	90	106.913(1)	90	642.38(1)	This work
$MgMo_{0.9}W_{0.1}O_4$	Sanmartinite	10.279 76(7)	9.293 31(8)	7.031 25(4)	90	106.935(1)	90	642.59(2)	This work
$MgMo_{0.5}W_{0.5}O_4$	Cuproscheelite	9.689 2(1)	6.945 33(7)	8.363 7(1)	101.741(1)	96.343(1)	107.085(1)	517.95(2)	This work
	Wolframite	4.687 6(2)	5.674 8(3)	4.924 9(2)	90	90.671(4)	90	131.00(2)	
$MgMo_{0.3}W_{0.7}O_4$	Cuproscheelite	9.689 0(2)	6.944 22(10)	8.363 2(2)	101.747(1)	96.343(1)	107.081(1)	517.83(3)	This work
	Wolframite	4.687 84(3)	5.674 77(4)	4.925 58(3)	90	90.685(1)	90	131.023(3)	
$MgMo_{0.1}W_{0.9}O_4$	Cuproscheelite	9.685 0(7)	6.940 8(4)	8.362 4(6)	101.712(4)	96.399(3)	107.077(4)	517.3(1)	This work
	Wolframite	4.688 04(2)	5.674 72(3)	4.926 92(2)	90	90.705(1)	90	131.062(2)	
$MgWO_4$	Wolframite	4.688 92(2)	5.675 29(3)	4.928 91(2)	90	90.726(1)	90	131.153(2)	This work
β-$MgMoO_4$	Sanmartinite	10.281	9.291	7.03	90	106.9	90	642.4	PDF 21-961
β-$MgMoO_4$	Sanmartinite	10.273(3)	9.288(3)	7.025(2)	90	106.96	90	641	[33]
α-$MgMoO_4$	Cuproscheelite	9.651	6.920	8.354	101.42	96.28	106.56	516	PDF 31-796
$MgMoO_4$[a]	Wolframite	4.66	5.64	4.84	90	90	90	127.7	PDF 16-308
$MgWO_4$	Wolframite	4.687 9	5.675 1	4.928 8	90	90.7	90	131.1	PDF 27-789
$MgWO_4$	Wolframite	4.686 4(4)	5.675 5(5)	4.928 4(4)	90	89.32	90	131	[34]
$MgWO_4$	Wolframite	4.695(1)	5.683 4(4)	4.937 1(7)	90	90.93(2)	90	131.72	[30]

[a] High-pressure phase.

of diffraction maxima with intermediate and a high intensities are present in the XRD pattern. However, all attempts to classify the extra phase(s) remained unsuccessful.

The values of the lattice parameters of different phases in the $MgMoO_4$–$MgWO_4$ system, obtained by full-profile Rietveld refinement of the patterns measured in the region $15° < 2\theta < 100°$ and corrected using peak positions of a Si standard are collected in table 2. For comparison, available literature data for the 'pure' $MgMoO_4$ and $MgWO_4$ structures are given too. In comparison with $MgMoO_4$, a small increase in the lattice parameters and the cell volume is observed for the $MgMo_{0.95}W_{0.05}O_4$ and $MgMo_{0.9}W_{0.1}O_4$ samples, in accordance with increasing average ionic radii of the tetrahedrally coordinated Mo^{6+} and W^{6+} species (0.41 Å and 0.42 Å, respectively, according to the Shannon scale [32]). Somewhat overestimated values of the cell dimensions are observed only for a 1%-doped $MgMo_{0.99}W_{0.01}O_4$ specimen.

From results of the phase and structural analyses it is evident that a $MgMo_{1-x}W_xO_4$ solid solution with a β-$MgMoO_4$ sanmartinite-type structure is formed in the $MgMoO_4$–$MgWO_4$ pseudo-binary system and its homogeneity spans (for the present conditions of synthesis) about 10 at.% of W. The range of existence of the solid solution with a β-$MgWO_4$ wolframite structure is narrower: the fraction of Mo substitution for W in the $MgWO_4$ structure is well below 10 at.%.

4. Luminescence and scintillation properties

The main goal of this study is to examine the potential of the $MgMoO_4$–$MgWO_4$ system for application in low-temperature scintillation detection of ionizing radiation and in x-ray luminescence techniques is the most relevant for this purpose. Firstly, it allows excitation of inner electron shells

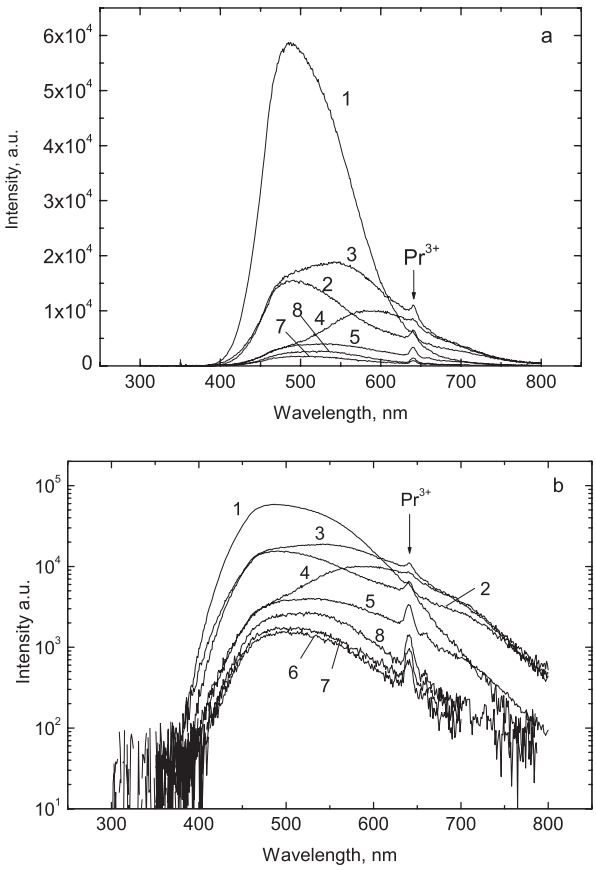

Figure 2. X-ray luminescence spectra of $MgMoO_4$–$MgWO_4$ compounds displayed in linear (a) and logarithmic (b) scales. (1) $MgWO_4$; (2) $MgMo_{0.1}W_{0.9}O_4$; (3) $MgMo_{0.5}W_{0.5}O_4$; (4) $MgMo_{0.7}W_{0.3}O_4$; (5) $MgMo_{0.9}W_{0.1}O_4$; (6) $MgMo_{0.95}W_{0.05}O_4$; (7) $MgMo_{0.99}W_{0.01}O_4$; (8) $MgMoO_4$ ($T = 8$ K).

of the constituent atoms, covering the energy range of our main interest. Secondly, due to the high penetration depth of the x-ray photons the observed emission is hardly sensitive to surface phenomena [35–37]. Consequently, the bulk emission properties are little affected by the excitation conditions, in contrast to experiments that use ultraviolet (UV) or vacuum ultraviolet (VUV) excitation, where this effect can be a serious concern.

Figure 2 shows the x-ray luminescence spectra of the compounds measured at a temperature of 8 K. They exhibit broadband emission in the yellow–red spectral range that can be attributed to the emission of tungstate and/or molybdate groups. A distinctive line at 640 nm was detected in the luminescence spectra of all studied samples. Judging from the spectral position of the line we deduced that it should be due to the emission of Pr^{3+} [1]. Indeed, the experimental samples were synthesized in a furnace that had been used for synthesis of praseodymium compounds, and this caused the inadvertent contamination. Fortunately the line emission of the rare-earth ions can be easily identified and excluded from the analysis of the luminescence data.

A pure magnesium molybdate exhibits a luminescence band of asymmetrical shape with a maximum at 520 nm. The position and shape of this band are consistent with those detected in single-crystalline β-$MgMoO_4$ at VUV and

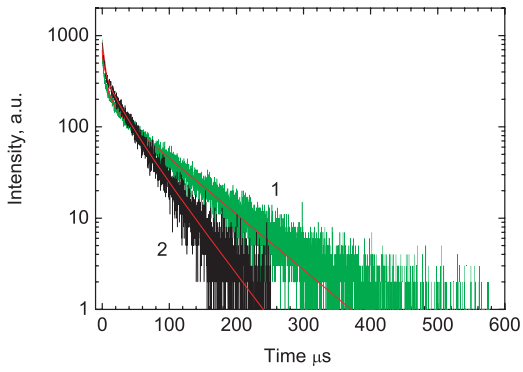

Figure 3. Scintillation decay curves of $MgWO_4$ measured at $T = 9$ K (1) and 300 K (2). The curves show the two-exponential fits to the experimental data.

(This figure is in colour only in the electronic version)

laser excitation [24, 38]. Figure 2 shows that the x-ray luminescence spectra of mixed $MgMo_{1-x}W_xO_4$ are very similar to that of $MgMoO_4$, while the emission intensity is inferior compared with pure magnesium molybdate in the range of low concentration ($x \leqslant 0.05$). As the content of tungsten in the system increases further, the emission intensity begins to rise and the spectral shape changes gradually. $MgMo_{0.9}W_{0.1}O_4$ exhibits a slightly higher light output than $MgMoO_4$ and one notices an increase in the light yield in the long-wavelength part of the spectrum.

With further increase of the tungsten content the luminescence band at 590 nm appears. This band dominates in the emission spectrum of the sample with 30 at.% tungsten. Based on the results of structure analysis we suggest that the band with a maximum at 600 nm is the characteristic emission of the cuprosheelite α-phase of $MgMoO_4$. The crystal structure is a key factor governing the emission properties of the material and it is worthwhile noting that $ZnMoO_4$ with the same crystal structure exhibits its main emission band at around 610 nm [39]. The luminescence data indicate that this phase begins to form in the system at $x = 0.1$. This observation demonstrates that the luminescence data allow to distinguish an admixture of another phase prior to it being sensed by means of conventional XRD analysis.

The long-wavelength emission band due to cuprosheelite α-$MgMoO_4$ remains noticeable even at a tungsten concentration as high as 90 at.%. As the concentration of tungsten approaches 50 at.% the sanmartinite β-phase of $MgWO_4$ with a wolframite structure is formed. This phase yields an emission band at about 490 nm that has an immediate effect on the luminescence of the sample under test. The intensity of the long-wavelength part gradually decreases with W concentration and the emission maximum shifts towards shorter wavelengths. Finally, pure $MgWO_4$ exhibits a very intense emission at 490 nm ($T = 8$ K), which is a characteristic luminescence of this phosphor material [1, 23]. This sample was used for studies of scintillation characteristics.

The temperature dependence of the scintillation decay of $MgWO_4$ was investigated from 300 to 9 K under excitation with α-particles. The best fit to the experimental data was achieved using a sum of two exponentials (see figure 3). The

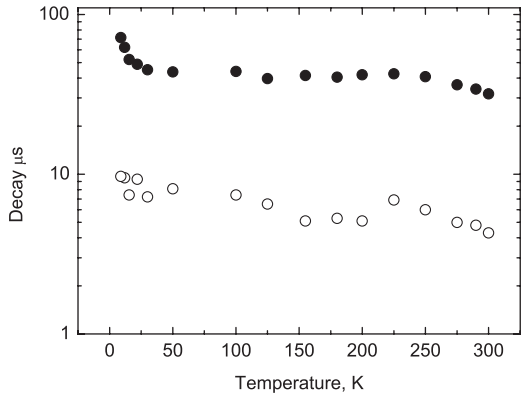

Figure 4. Temperature dependence of the fast (open symbol) and slow (solid symbol) decay time constants of $MgWO_4$ obtained from a two-exponential fit. Excitation with an α-source (^{241}Am).

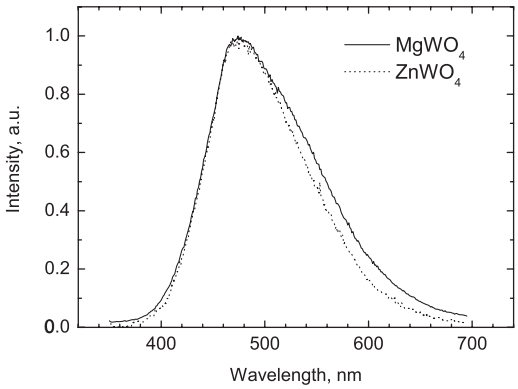

Figure 5. Normalized x-ray luminescence spectra of $MgWO_4$ and $ZnWO_4$ ($T = 295$ K).

values of decay time constants are found to be as follows: $\tau_1 = 4.3$, $\tau_2 = 31.9$ μs at $T = 300$ K and $\tau_1 = 9.7$, $\tau_2 = 71.9$ μs at $T = 9$ K. The variation of decay time constants with temperature, presented in figure 4, demonstrates that the thermal quenching has only a very modest effect on the luminescence. The decay kinetics changes very little with cooling of the sample, indicating that the non-radiative decay processes are not effective up to room temperature. This is consistent with the high temperature of luminescence quenching observed in $MgWO_4$ ($T = 400$ K) [8]. A rapid increase of the decay time constant that starts at low temperatures ($T < 30$ K) is another characteristic feature of the intrinsic emission of tungstates: it is associated with the energy structure of the emitting centre that contains a metastable level a few meV below the emitting one [9, 29, 40].

Finally, we endeavour to evaluate the scintillation efficiency of $MgWO_4$. The x-ray luminescence spectra of $MgWO_4$ and $ZnWO_4$ were measured at $T = 295$ K and it was found that they have very similar spectral distributions (see figure 5). The emission maximum of both materials is located at 480 nm, agreeing well with reference data [1, 41]. Therefore, the relative comparison of the emission efficiency of these compounds is straightforward in spite of a spectrally selective response of the detector used (photomultiplier tube). In such a way, the relative light output of the $MgWO_4$ sample at room temperature was found to be equal (0.90 ± 0.15) to that of the $ZnWO_4$ reference sample used previously for comparative analysis of scintillation powder [42].

5. Discussion

Though luminescence of $MgWO_4$ was first characterized a few decades ago [5, 8] and has been used for a while as a commercial phosphor [1, 23], further studies of the material properties are rare [41, 43]. The results of physical–chemical characterization of $MgMoO_4$ were published several years ago [44], while optical and luminescence properties were investigated very recently [24, 38].

It is now well established that the transitions responsible for excitation and emission in tungstate and molybdate are due to the electronic transitions of a charge-transfer type[6] within the oxyanion complex $[MeO_n]$ [9]. Calculations of the electronic structure of the crystals confirmed that the upper occupied states have mostly O2p character and the lower unoccupied band is mainly made of d-states of the cation [45–48]. Therefore, to account for the luminescence properties of tungstates and molybdates, emphasis is usually placed on the coordination number and the geometry of this complex. In the case of an isolated group the configuration coordination diagram is a valid approach. The emission colour is determined by the position of the lowest-energy excitation (absorption) band and the magnitude of the Stokes shift.

Table 3 summarizes the results of the present studies of the $MgMoO_4$–$MgWO_4$ system, allowing us to identify three main types of structure with their characteristic luminescence features. Let us consider the effect of structure on the emission of two different phases of molybdates. Inspection of this table shows that the position of the emission peak is very strongly influenced by the symmetry and closest surroundings of the emission centre. The lower the symmetry of the emission centre the larger the Stokes shift. The oxyanion complex in β-$MgMoO_4$ has four-fold coordination with small distortion (the deviation from the average distance $d_{Mo-O} = 1.76$ Å is about 2.8%). On the other side α-$MgMoO_4$ exhibits the highest Stokes shift, and according to the structural data there are two types of Mo-site[7]. The first type is the slightly distorted MoO_4 tetrahedron (deviation from the average distance $d_{Mo-O} = 1.77$ Å is ca 2.3%). Two other sites can be considered as an oxyanion group in four-fold coordination (average distances $d_{Mo-O} = 1.77$ and 1.76 Å, deviation 1.1 and 3.4%) having one more oxygen atom in close proximity (see figure 6). This oxygen imposes an extra repulsive potential on the electron that occupies the Mo 4d orbital in the excited state. That can also be explained in terms of the crystal field effect of oxygen on d-state of Mo in the $[MoO_4]^{2-}$ centre [49]. In turn this causes lowering of the energy level of the excited state and

[6] Though in reality the transitions involve reorganization of the electronic charge of the metal and oxygen without a considerable amount of real transfer of the charge it remains a good approximation, especially for illustrative purposes.

[7] The existence of two different emission sites is also suggested for $ZnMoO_4$ that has the same crystal structure as α-$MgMoO_4$ [39].

Table 3. Luminescence ($T = 8$ K) and structural data for $MgMoO_4$–$MgWO_4$ system.

Compound	Symmetry	Emission max, nm (eV)	Excit. onset (eV)	Stokes shift (eV)	Quenching temp. (K)	Average Me–O distance (Å)	Coordin. number	Average Me–Me distance (Å)
β-$MgMoO_4$	$C2/m$	520 (2.40)	3.9 [24]	1.55	30 [24]	1.76 ± 0.05	4	4.67 ± 0.35
α-$MgMoO_4$	$P\bar{1}$	600 (1.95)	4.0 [a] [39]	2.05	200 [a] [39]	1.77 ± 0.04 [b] 1.77 ± 0.02 & 2.79 [b] 1.76 ± 0.06 & 3.07 [b]	4 4 & 1 4 & 1	4.55 ± 0.32
$MgWO_4$ (wolframite)	$P2/c$	490 (2.45)	4.0 [41]	1.5	400 [9]	1.94 ± 0.05	6	4.31 ± 0.25

[a] Data for $ZnMoO_4$.

[b] Corresponding distances were calculated from the refined values of the lattice parameters of cuprosheelite phases given in table 2 and atomic coordinates in $ZnMoO_4$ from [31].

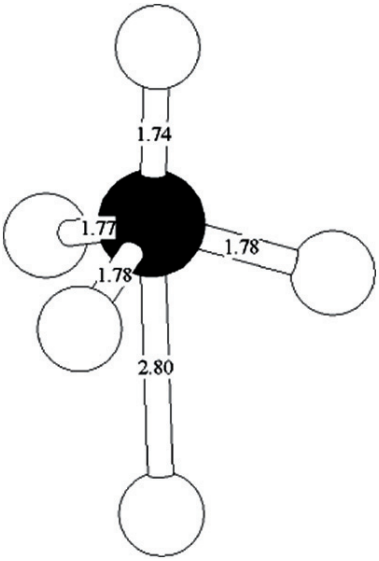

Figure 6. Model of the MoO_4 tetrahedron in the α-$MgMoO_4$ structure that also shows a fifth oxygen atom in close proximity ($d_{Mo-O} = 2.80$ Å).

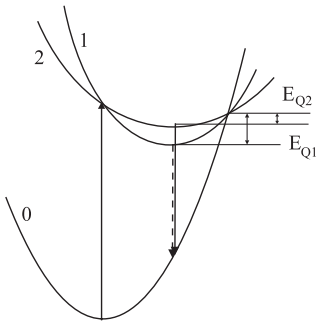

Figure 7. Schematic configuration coordination diagram of the MoO_4 oxyanion complex in the ground (0) and excited states (1, 2) in α-$MgMoO_4$ (1) and β-$MgMoO_4$ (2) structures. The scheme demonstrates the relation between the emission energy E_{em} and quenching activation energy E_q in the case of the emission centre exhibiting different APES slopes in the excited state.

subsequently a larger Stokes shift of the emission. In some way this is equivalent to the effect of the low symmetry on the emission centre observed, for example in $Bi_4Ge_3O_{12}$, that has a highly asymmetric Bi^{3+} site and exhibits an unusually large Stokes shift [23].

The configuration coordination diagram very effectively demonstrates the difference in the luminescence properties of the two phases of magnesium molybdate. Judging from the similarity of the structure of the $[MoO_4]$ cluster, it is reasonable to assume that the adiabatic potential energy surfaces (APES) of the ground state for the $[MoO_4]^{2-}$ emission centre in α- and β-$MgMoO_4$ should have very similar shapes. Thus, based on spectroscopic results compiled in table 3, one can suggest that the main difference in the configuration coordination diagrams should be the magnitude of the force constant (k) of the excited state, which defines the slope of APES in this state [50]. The value of k should be higher for the $[MoO_4]^{2-}$ centre in α-$MgMoO_4$ that experiences additional Coulomb interaction with the neighbouring oxygen. Figure 7 shows the corresponding configuration coordinate diagram for α- and β-$MgMoO_4$ and graphically demonstrates the reason for the different Stokes shifts.

It should be noted that this model is also helpful for understanding the observed difference in the luminescence quenching temperature of two molybdates. Such a non-radiative quenching process in terms of a configuration coordination diagram is a return from the excited state to the ground state through the crossing point of their APES. It is clear from the figure that the activation energy E_Q which is necessary to reach the cross-over point of the APES of excited and ground states is lower for excited state 2 compared with that of excited state 1 ($E_{Q2} < E_{Q1}$). Therefore, compound 1, with the larger Stokes shift, should be less affected by the quenching process. Qualitatively this agrees well with our findings for the two types of magnesium molybdate structures: cuproscheelite α-$MgMoO_4$ exhibits luminescence with a significantly larger Stokes shift and consequently much higher quenching temperature in comparison with that of sanmartinite β-$MgMoO_4$.

Regarding magnesium tungstate, the small magnitude of distortion of the WO_6 octahedron can account for a similar value of the Stokes shift as seen for β-$MgMoO_4$. However, these materials are completely different in terms of luminescence intensity and therefore this approach cannot be used in a straightforward way for comparison. The significant discrepancy in the structure of the oxyanion complex and the cation–anion interaction in ground and excited states can strongly influence the luminescence properties and must be considered quantitatively. Reassuringly, the feasibility

of calculation techniques for the studies of this issue in wolframite tungstates has recently been demonstrated [51].

6. Summary

The search for cryogenic scintillation materials motivated our interest in the $MgMoO_4$–$MgWO_4$ system. We synthesized a series of samples and examined their structural, luminescence and scintillation properties. From the structural point of view, the $MgMoO_4$–$MgWO_4$ pseudo-binary system comprises three main types of structure: sanmartinite β-$MgMoO_4$, cuproscheelite α-$MgMoO_4$ and wolframite $MgWO_4$. The single-phase mixed solid solution of $MgMo_{1-x}W_xO_4$ with a β-$MgMoO_4$ structure is created only at $x < 0.10$, while at higher tungsten contents a mixture of different phases is formed.

The results of x-ray luminescence studies are very consistent with these findings. The luminescence spectra of $MgMo_{1-x}W_xO_4$ resemble these of pure sanmartinite β-$MgMoO_4$. As the W/Mo ratio changes within the range 0.1–0.9 the luminescence spectra vary consistently, exhibiting three principal emission bands at 520, 590 and 490 nm which are attributed to three main phases β-$MgMoO_4$, α-$MgMoO_4$ and wolframite $MgWO_4$, respectively. These studies showed that W substituting for Mo in the range of concentration where the mixed solid solution $MgMo_{1-x}W_xO_4$ is formed does not yield an increase of the light output of the compound. The moderate improvement of the emission efficiency at higher concentrations of W is due to the appearance of other phases that obviously would preclude the production of a single crystal. Pure $MgWO_4$ is found to be the only material that manifests favourable emission properties, and this sample was subjected to scintillation characterization. The scintillation response of $MgWO_4$ was compared with that of $ZnWO_4$ and the ratio of the light yield was found to be 0.90 ± 0.15. Since the scintillation response of $MgWO_4$ does not deteriorate with cooling, this estimate is quite encouraging: it shows that from the viewpoint of detection efficiency $MgWO_4$ has very good chances of being considered as a cryogenic scintillation detector, provided that single crystals can be produced.

Acknowledgments

The work was supported in part by a grant from the Royal Society (London) 'Development of advanced crystal scintillators for cryogenic dark matter experiment'.

References

[1] Shionoya S and Yen W M (ed) 1999 *Phosphor Handbook* (Boca Raton, FL: CRC Press)
[2] Derenzo S E and Moses W W 1993 Experimental efforts and results in finding new heavy scintillators *Heavy Scintillators for Scientific and Industrial Applications* ed F De Notaristefani, P Lecoq and M Schneegans (Gif-sur-Yvette: Frontieres) p 125
[3] Globus M, Grinyov B and Kim J K 2005 *Inorganic Scintillators for Modern and Traditional Applications* (Kharkov: Institute for Single Crystals Press)
[4] Kaminskii A A 1981 *Laser Crystals* (Berlin: Springer)
[5] Kröger F A 1948 *Some Aspects of the Luminescence of Solids* (New York: Elsevier)
[6] Botden Th P J 1951 *Phil. Res. Rep.* **6** 425
[7] van Loo W 1975 *Phys. Status Solidi* a **25** 565
[8] Tyner C E and Drickamer H G 1977 *J. Chem. Phys.* **67** 4103
[9] Blasse G 1980 *Struct. Bond.* **42** 1
[10] Grasser R, Pitt E, Shrarmann A and Zimmerer G 1975 *Phys. Status Solidi* b **69** 359
[11] Reut E G 1985 *Izv. Akad. Nauk SSSR Ser. Fiz.* **49** 2032 (in Russian)
[12] Errandonea D, Martínez-García D, Lacomba-Perales R, Ruiz-Fuertes J and Segura A 2006 *Appl. Phys. Lett.* **89** 091913
[13] Lecoq P *et al* 1995 *Nucl. Instrum. Methods* A **365** 291
[14] Annenkov A A, Korzhik M V and Lecoq P 2002 *Nucl. Instrum. Methods* A **490** 30
[15] Kraus H *et al* 2006 *J. Phys. Conf. Ser.* **39** 139
[16] Westphal W *et al* 2006 *Czech. J. Phys.* **56** 535
[17] Pirro S, Arnaboldi C, Beeman J W and Pessina G 2006 *Nucl. Instrum. Methods* A **559** 361
[18] de Marcillac P, Coron N, Dambier G, Leblanc J and Moalic J-P 2003 *Nature* **422** 876
[19] Cozzini C *et al* 2004 *Phys. Rev.* C **70** 064606
[20] Alessandrello A *et al* 1998 *Phys. Lett.* B **420** 109
[21] Bravin M *et al* 1999 *Astropart. Phys.* **12** 107
[22] Mikhailik V B and Kraus H 2006 *J. Phys. D: Appl. Phys.* **39** 1181
[23] Blasse G and Grabmaier B C 1994 *Luminescent Materials* (Berlin: Springer)
[24] Mikhailik V B, Kraus H, Wahl D and Mykhaylyk M S 2005 *Phys. Status Solidi* b **242** R17
[25] Pirro S 2007 private communication
[26] Akselrud L G *et al* 1993 *Mater. Sci. Forum.* **133–136** 335
[27] Kraus H, Mikhailik V B and Wahl D 2005 *Nucl. Instrum. Methods* A **553** 522
[28] Kraus H, Mikhailik V B and Wahl D 2007 *Radiat. Meas.* **42** 921
[29] Mikhailik V B, Kraus H, Henry S and Tolhurst A J B 2007 *Phys. Rev.* B **75** 184308
[30] Macavei J and Schulz H 1993 *Z. Kristallogr.* **207** 193
[31] Abrahams S C 1967 *J. Chem. Phys.* **46** 2052
[32] Shannon R D 1976 *Acta Crystallogr.* A **32** 751
[33] Bakakin V V, Klevtsova R F and Gaponenko L A 1982 *Kristallografiya* **27** 38
[34] Filipenko O S, Pobedimskaya E A, Ponomarev V I and Belov N V 1968 *Kristallografiya* **13** 1073
[35] Benitez E L, Husk D E, Schnatterly S E and Tario C 1991 *J. Appl. Phys.* **70** 3256
[36] Elango M 1994 *Radiat. Eff. Defects Solids* **128** 1
[37] Mikhailik V B, Kraus H, Miller G, Mykhaylyk M S and Wahl D 2005 *J. Appl. Phys.* **97** 083523
[38] Mikhailik V B, Kraus H, Itoh M, Iri D and Uchida M 2005 *J. Phys.: Condens. Matter* **17** 7209
[39] Mikhailik V B, Kraus H, Wahl D, Ehrenberg H and Mykhaylyk M S 2006 *Nucl. Instrum. Methods* A **562** 513
[40] Babin V *et al* 2004 *Radiat. Meas.* **38** 503
[41] Kolobanov V N *et al* 2002 *Nucl. Instrum. Methods* A **486** 496
[42] Kraus H *et al* 2007 *Phys. Status Solidi* a **204** 730
[43] Chu J P, Hsieh I J, Chen J T and Feng M S 1998 *Mater. Chem. Phys.* **53** 172
[44] Rodriguez J A, Hanson J C, Chaturvedi S, Maiti A and Brito J L 2000 *J. Chem. Phys.* **112** 935
[45] Zhang Y, Holthwarth N A W and Williams R T 1998 *Phys. Rev.* B **57** 12738
[46] Itoh M, Fujita N and Inabe Y 2006 *J. Phys. Soc. Japan* **75** 084705
[47] Hizhnyi Yu A, Nedilko S G and Nikolaenko T N 2005 *Nucl. Instrum. Methods* A **537** 36
[48] Fujita M *et al* 2008 *Phys. Rev.* B **77** 155118
[49] Abraham Y B, Holzwarth N A, Williams R T, Matthews G E and Tacett A R 2001 *Phys. Rev.* B **64** 245109
[50] Saito N, Sonoyama N and Sakata T 1996 *Bull. Chem. Soc. Japan* **69** 2191
[51] Hizhnyi Yu A, Nikolaenko T N and Nedilko S G 2007 *Phys. Status Solidi* c **4** 1217